UMD
MARYLAND

COLLEGE PARK CAMPUS

Determining Conductivity by Boundary Measurements: Some Numerical Results

In-Ja B. Lee
Institute for Physical Science and Technology
University of Maryland
College Park, Maryland 20742

Technical Note BN-1076

May 1988

INSTITUTE FOR PHYSICAL SCIENCE AND TECHNOLOGY

Encl (1)

SECURITY CLASSIFICATION OF THIS PAGE (When Data Entered)

REPORT DOCUMENTATION PAGE		READ INSTRUCTIONS BEFORE COMPLETING FORM
1. REPORT NUMBER BN-1076	2. GOVT ACCESSION NO.	3. RECIPIENT'S CATALOG NUMBER
4. TITLE (and Subtitle) Determining Conductivity by Boundary Measurements: Some Numerical Results		5. TYPE OF REPORT & PERIOD COVERED Final life of the contract 6. PERFORMING ORG. REPORT NUMBER
7. AUTHOR(s) In-Ja B. Lee		8. CONTRACT OR GRANT NUMBER(s) NSF DMS-8601490 ONR N00014-85-K-0169
9. PERFORMING ORGANIZATION NAME AND ADDRESS Institute for Physical Science and Technology University of Maryland College Park, MD 20742		10. PROGRAM ELEMENT, PROJECT, TASK AREA & WORK UNIT NUMBERS
11. CONTROLLING OFFICE NAME AND ADDRESS Department of the Navy Office of Naval Research Arlington, VA 22217		12. REPORT DATE May 1988 13. NUMBER OF PAGES 24
14. MONITORING AGENCY NAME & ADDRESS(if different from Controlling Office)		15. SECURITY CLASS. (of this report) 15a. DECLASSIFICATION/DOWNGRADING SCHEDULE

16. DISTRIBUTION STATEMENT (of this Report)

Approved for public release: distribution unlimited

17. DISTRIBUTION STATEMENT (of the abstract entered in Block 20, if different from Report)

18. SUPPLEMENTARY NOTES

19. KEY WORDS (Continue on reverse side if necessary and identify by block number)

20. ABSTRACT (Continue on reverse side if necessary and identify by block number)

We consider the problem of determining an unknown conductivity by boundary measurements. First we briefly review various known results about uniqueness and continuous dependence. The main emphasis of this paper is on the discussion of some numerical results for a variational algorithm to recover the conductivity.

DD FORM 1 JAN 73 1473 EDITION OF 1 NOV 65 IS OBSOLETE

S/N 0102-LF-014-6601

SECURITY CLASSIFICATION OF THIS PAGE (When Data Entered)

Determining Conductivity by Boundary Measurements: Some Numerical Results

IN-JA B. LEE†

Abstract. We consider the problem of determining an unknown conductivity by boundary measurements. First we briefly review various known results about uniqueness and continuous dependence. The main emphasis of this paper is on the discussion of some numerical results for a variational algorithm to recover the conductivity.

1. Introduction. We study the following inverse problem: can one determine an unknown conductivity $\gamma(x)$ inside a body Ω by means of measurements of potential and flux on the boundary? This problem was first raised by Calderón and has since been studied by several people.

In the following Ω will be a bounded C^∞ domain in $\mathbf{R}^n$, $n \geq 2$, with boundary Γ. The unknown conductivity $\gamma(x)$ is in $L^\infty(\Omega)$ and satisfies $0 < \gamma_0 \leq \gamma(x)$ for all $x \in \Omega$. Consider the operator

$$L_\gamma(u) = \nabla \cdot (\gamma(x) \nabla u)$$

acting on $H^1(\Omega)$.

We define the Dirichlet to Neumann-data map

$$\Lambda_\gamma : H^{1/2}(\Gamma) \to H^{-1/2}(\Gamma) \qquad \text{by}$$
$$\Lambda_\gamma(\phi) = \gamma \frac{\partial u}{\partial \nu},$$

where u solves the following boundary value problem

$$\begin{aligned} L_\gamma u &= 0 \quad \text{in} \quad \Omega, \\ u &= \phi \quad \text{on} \quad \Gamma. \end{aligned} \tag{1.1}$$

The inverse problem now is to determine γ given knowledge of $\Lambda_\gamma(\phi)$. We say that γ is identifiable if the map $\gamma \mapsto \Lambda_\gamma$ is injective. In section 2 we briefly review known results concerning the identifiability of γ. Section 3 concerns the question of continuous dependence. In the last three sections of this paper, we study a particular algorithm to determine γ; the emphasis is on the presentation of various numerical experiments.

†Department of Mathematics, University of Maryland, College Park, Maryland 20742. Supported by NSF grant DMS-8601490 and ONR contract N00014-85-K-0169.

2. Identifiability Results. For many purposes it is more convenient to work with the energies

$$Q_\gamma(\phi) = \int_\Omega \gamma |\nabla u|^2 \, dx,$$

instead of the operator Λ_γ. It is easy to see that knowing $Q_\gamma(\phi)$, for any $\phi \in H^{1/2}(\Gamma)$, is equivalent to knowing Λ_γ.

Kohn and Vogelius [5] proved that γ is uniquely determined by $Q_\gamma(\phi)$ if γ is analytic.

THEOREM(KOHN–VOGELIUS). *Let γ_i, $i = 1, 2$, be in $L^\infty(\Omega)$ with a positive lower bound. Let $x_0 \in \Gamma$ and let B be a neighborhood of x_0 relative to $\bar{\Omega}$. Suppose*

$$\gamma_i \in C^\infty(B), \qquad \text{for} \quad i = 1, 2$$

and

$$Q_{\gamma_1}(\phi) = Q_{\gamma_2}(\phi) \qquad \text{whenever} \quad \phi \in H^{1/2}(\Gamma) \quad \text{with} \quad \text{supp}\, \phi \subset B \cap \Gamma.$$

Then

$$D^k \gamma_1(x_0) = D^k \gamma_2(x_0), \qquad \text{for all} \quad k = (k_1, \cdots, k_n) \geq 0,$$

where D^k denotes the derivative $(\partial/\partial x_1)^{k_1} \cdots (\partial/\partial x_n)^{k_n}$.

The main trick in the proof of this theorem is to take boundary data ϕ that are highly oscillatory, with vanishing moments and supported in a small neighborhood of $x_0 \in \Gamma$. For such ϕ, the solution of (1.1) will decay rapidly away from x_0; these ϕ are therefore well suited for studying γ at x_0. The following three lemmas are the main ingredients of the proof of the theorem.

LEMMA 1. *Let M be any positive integer, and let z be a point on Γ. There exists a sequence $\{\phi_N\}_{N=1}^\infty \subset C^\infty(\Gamma)$ such that*

$$\|\phi_N\|_{1/2+t,\Gamma} \leq C_t N^t, \qquad t \geq -M$$

$$\|\phi_N\|_{1/2,\Gamma} = 1,$$

$$\text{supp}\, \phi_N \downarrow \{z\} \qquad \text{as} \quad N \to \infty.$$

Fix M_0 and let u_N denote the solution to the boundary value problem

$$\begin{aligned} L_\gamma u_N &= 0 \qquad \text{in} \quad \Omega, \\ u_N &= \phi_N \qquad \text{on} \quad \Gamma, \end{aligned}$$

where the sequence $\{\phi_N\}_{N=1}^\infty$ is as in lemma 1 with $M = M_0$.

LEMMA 2. *Let $\Omega' \subset \Omega$ with dist $(z, \Omega') > 0$, and assume that γ is in C^∞ in a neighborhood of z. Then*

$$\|u_N\|_{1,\Omega'} \leq C N^{-M_0}$$

for all $N \geq 1$. The constant C depends on $\gamma, \Omega', z,$ and M_0, but not on N.

Define

$$\rho(x) = \text{dist } (x, \Gamma) \qquad \text{for any } x \in \Omega.$$

LEMMA 3. *Assume that γ is C^∞ in a neighborhood of z, and let U denote any neighborhood of z. Given $l \geq 0$ and $\epsilon > 0$, there exists a constant $C_{l,\epsilon} > 0$ such that*

$$\int_U \rho(x)^l |\nabla u_N|^2 \, dx \geq C_{l,\epsilon} N^{-(n+\epsilon)l}$$

for sufficiently large N.

Sketch of the proof of Theorem: the proof proceeds by contradiction using the three lemmas. If the theorem were not true, we may suppose that

$$\gamma_1(x) - \gamma_2(x) \geq C \rho(x)^l, \qquad x \in U,$$

for some constant $C > 0$ and some neighborhood U of a point $z \in \Gamma$, arbitrarily close to x_0. Choose $M_0 > \frac{1}{2} nl$. Let u_N^i, $i = 1, 2$, solve

$$L_{\gamma_i} u_N^i = 0, \qquad u_N^i|_\Gamma = \phi_N.$$

Then, for sufficiently large N,

$$\begin{aligned}
\int_\Omega \gamma_1 |\nabla u_N^1|^2 \, dx &\geq \int_U \gamma_2 |\nabla u_N^1|^2 \, dx + C \int_U \rho(x)^l |\nabla u_N^1|^2 \, dx \\
&\geq \int_\Omega \gamma_2 |\nabla u_N^1|^2 \, dx - \int_{\Omega \setminus U} \gamma_2 |\nabla u_N^1|^2 \, dx + C_{l,\epsilon} N^{-(n+\epsilon)l} \\
&\geq \int_\Omega \gamma_2 |\nabla u_N^2|^2 \, dx - C N^{-2M_0} + C_{l,\epsilon} N^{-(n+\epsilon)l}.
\end{aligned}$$

Since $2M_0 > nl$, we get

$$\int_\Omega \gamma_1 |\nabla u_N^1|^2 \, dx > \int_\Omega \gamma_2 |\nabla u_N^2|^2 \, dx,$$

for all sufficiently large N, and this is a contradiction. □

Kohn and Vogelius [7] have extended their study to piecewise analytic γ showing that it is possible to determine an unknown conductivity interior to a body Ω from measurements of the potential and the flux on the boundary.

Sylvester and Uhlmann [10] have subsequently shown the uniqueness result in the more difficult case $\gamma \in C^\infty(\Omega)$.

THEOREM(SYLVESTER–UHLMANN). *Let $\Omega \subset \mathbf{R}^n$ $(n \geq 3)$ be a domain with smooth boundary. Suppose γ_0 and γ_1 are in $C^\infty(\bar{\Omega})$, $\gamma_0, \gamma_1 > 0$ in $\bar{\Omega}$ and*

$$Q_{\gamma_0}(\phi) = Q_{\gamma_1}(\phi) \qquad \forall \phi \in H^{1/2}(\Gamma)$$

then

$$\gamma_0 = \gamma_1 \qquad in \quad \Omega.$$

This theorem has been established only for space dimension greater than or equal to three. It is not known whether the same result holds for space dimension two. But in that case Sylvester and Uhlmann [9] have obtained a local uniqueness result for coefficients that are nearly constant in $C^\infty(\Omega)$.

So far, we only have considered scalar coefficients γ corresponding to isotropic conductors. It is also of practical importance to study symmetric matrix valued coefficients

$$\gamma_{ij} = \gamma_{ji} \in L^\infty(\Omega)$$
$$\lambda|\xi|^2 \leq (\gamma(x)\xi, \xi) \leq \frac{1}{\lambda}|\xi|^2 \qquad \text{for all } x \in \Omega \text{ and } \xi \in \mathbf{R}^n.$$

In this case we can not expect to recover the full matrix $\{\gamma_{ij}\}$. If two matrix conductivities γ and δ are related by change of variables

$$\delta_{kl}(\Phi(x)) = |\det D\Phi|^{-1} \sum_{i,j} \gamma_{ij}(x) \frac{\partial \Phi_k}{\partial x_i} \frac{\partial \Phi_l}{\partial x_j}$$

(Φ is a diffeomorphism of Ω), then u solves (1.1) with coefficient γ if and only if $u^\Phi = u o \Phi^{-1}$ solves the similar problem with coefficient δ. If, in addition,

$$\Phi(x) = x \qquad \text{for} \quad x \in \Gamma,$$

then $u^\Phi = u$ on Γ, and

$$\gamma \nabla u \cdot \nu = \delta \nabla u^\Phi \cdot \nu \quad \text{on} \quad \Gamma.$$

It therefore follows that γ and δ have identical boundary measurements. Concerning uniqueness Kohn and Vogelius [6] have proved that if $(n-1)$ eigenvalues and eigenvectors of γ are known then the last eigenvalue can be distinguished by boundary measurements.

3. Continuous Dependence Results. It is very important to study the continuity properties of the mapping $\Lambda_\gamma \to \gamma$. We define the operator norm

$$\|\Lambda_\gamma\|_{1/2,-1/2} = \sup_{\phi \neq 0} \frac{\|\Lambda_\gamma(\phi)\|_{H^{-1/2}(\Gamma)}}{\|\phi\|_{H^{1/2}(\Gamma)}}.$$

Sylvester and Uhlmann [11] have recently shown

THEOREM(SYLVESTER–UHLMANN). *Suppose that γ_1 and γ_2 are measurable and satisfy, for some λ,*

$$0 < \frac{1}{\lambda} \leq \gamma_i \leq \lambda \qquad \text{for} \quad i = 1, 2$$

then

$$\|\Lambda_{\gamma_1} - \Lambda_{\gamma_2}\|_{1/2,-1/2} \leq C_1 \|\gamma_1 - \gamma_2\|_{L^\infty(\Omega)}.$$

If, in addition, γ_1 and γ_2 are continuous, then

$$\|\gamma_1 - \gamma_2\|_{L^\infty(\Gamma)} \leq C_2 \|\Lambda_{\gamma_1} - \Lambda_{\gamma_2}\|_{1/2,-1/2}.$$

Let $B_i = \Lambda_{\gamma_i} - \gamma_i \Lambda_1$. If, γ_1 and γ_2 are Lipschitz continuous, and for some β,

$$|\nabla \gamma_i| \leq \beta \qquad \text{for} \quad i = 1, 2,$$

then

$$\|B_1 - B_2\|_{1/2,-1/2} \leq C_3 \|\gamma_1 - \gamma_2\|_{W^{1,\infty}(\Omega)}$$

and

$$\|\gamma_1 - \gamma_2\|_{W^{1,\infty}(\Gamma)} \leq C_4 (\|B_1 - B_2\|_{1/2,-1/2} + \|\Lambda_{\gamma_1} - \Lambda_{\gamma_2}\|_{1/2,-1/2})$$

The constants C_i depend only on Ω, λ and β.

This result also can be proven by a simple modification of the method of Kohn and Vogelius. See for instance Alessandrini [1]. Alessandrini, furthermore, obtained the following result under the assumption that $\gamma_i, i = 1, 2$, satisfies a-priori inequalities

$$\frac{1}{\lambda} \leq \gamma_i(x), \qquad \text{for all } x \in \Omega$$
$$\|\gamma_i\|_{H^{s+2}(\Omega)} \leq \lambda, \qquad i = 1, 2$$

for some s and λ, $s \geq n/2$.

THEOREM(ALESSANDRINI). *With conditions as stated above,*

$$\|\gamma_1 - \gamma_2\|_{L^\infty(\Omega)} \leq \omega(\|\Lambda_{\gamma_1} - \Lambda_{\gamma_2}\|_{1/2,-1/2}),$$

and the function ω is such that

$$\omega(t) \leq C\, |\log t|^{-\delta}, \quad \forall t, \quad 0 < t < 1/e,$$

for some C, δ, $0 < \delta < 1$, depending only on λ, n and s.

This result is somewhat disappointing since it predicts such a weak form of continuous dependence. In its generality the result may, however, very well be the best possible.

It becomes quite natural to analyze continuous dependence for classes of conductivities with more restricted spatial dependence. For practical reasons, it is important to seek continuous dependence estimates in terms of finitely many sets of boundary measurements.

Friedman and Vogelius [4] studied conductivities that correspond to a finite number of small inhomogeneities, of extreme conductivity, imbeded in an n–dimensional reference medium. The reference conductivity γ is assumed to be $C^{2+\beta}$. Each inhomogeneity has the form $z_k + \epsilon\,\rho_k\,B$, where B is some bounded domain in $\mathbf{R}^n$, $n \geq 2$, with $0 \in B$ and ∂B of type $C^{2+\beta}$. The points $\{z_1, \cdots, z_k\}$ belong to Ω and satisfy

$$\begin{aligned} &|z_k - z_j| \geq d_0 > 0, \qquad \forall j \neq k \qquad \text{and} \\ &\text{dist}\,(z_k, \Gamma) \geq d_0, \qquad \forall k. \end{aligned}$$

Here ϵ is assumed to be small enough that the sets $\{z_k + \epsilon\rho_k B\}$ are disjoint and that their distance to $\mathbf{R}^n \backslash \Omega$ is larger than $\frac{d_0}{2}$. Ω is assumed to be bounded with boundary $\Gamma \in C^{2+\beta}$. Let

$$\omega_\epsilon = \bigcup_{k=1}^{K} (z_k + \epsilon\rho_k B)$$

denote the total collection of inhomogeneities. If they all have infinite conductivity, then the voltage potential u_ϵ, given the boundary current ψ, solves

$$\min_{u \in H^1(\Omega), \nabla u = 0 \text{ in } \omega_\epsilon} \{\frac{1}{2}\int_\Omega \gamma\,|\nabla u|^2\,dx - \int_\Gamma \psi u\,ds\}.$$

For this problem to have a unique solution we require that

$$\int_\Gamma \psi\,ds = 0 \qquad \text{and} \qquad \int_\Gamma u_\epsilon\,ds = 0.$$

Consider two arbitrary collections of inhomogeneities

$$\omega_\epsilon = \bigcup_{k=i}^{K} (z_k + \epsilon\rho_k B) \quad \text{and} \quad \omega'_\epsilon = \bigcup_{k=i}^{K'} (z'_k + \epsilon\rho'_k B),$$

and denote by u_ϵ and u'_ϵ the corresponding voltage potentials with fixed boundary current ψ. Let U denote the solution to

$$\min_{U \in H^1(\Omega)} \{\frac{1}{2}\int_\Omega \gamma\,|\nabla U|^2\,dx - \int_\Gamma \psi U\,ds\}.$$

It is important that U satisfy the non-degeneracy condition of $\nabla U \neq 0$.

THEOREM (FRIEDMAN–VOGELIUS). *Let Γ_1 be nonempty open subset of Γ. There exist constants $0 < \epsilon_0, \delta_0$ and C and a function $\eta(\epsilon)$, $\lim_{\epsilon \to 0} \eta(\epsilon) = 0$, such that if $\epsilon < \epsilon_0$ and $\epsilon^{-n} \|u_\epsilon - u'_\epsilon\|_{L^\infty(\Gamma_1)} < \delta_0$, then*

(1) *$K = K'$, and, after appropriate reordering,*

(2) $|z_k - z'_k| + |\rho_k - \rho'_k| \leq C\, \epsilon^{-n} \|u_\epsilon - u'_\epsilon\|_{L^\infty(\Gamma_1)} + \eta(\epsilon) \quad (1 \leq k \leq K)$.

The constants ϵ_0, δ_0 and C and the function η are independent of the two sets of inhomogeneities.

A similar result can be obtained for non-conducting inhomogeneities as well as for the case where the voltage potential ϕ is fixed and the current flux ψ is measured.

4. Numerical Algorithm. To build an algorithm to reconstruct the conductivity we consider the functional

$$F(\gamma, u, \sigma) = \int_\Omega |\gamma^{1/2} \nabla u - \gamma^{-1/2} \sigma|^2 \, dx. \tag{4.1}$$

It is clear that $F(\gamma, u, \sigma)$ is non-negative and that $F(\gamma, u, \sigma) = 0$ if and only if $\gamma^{1/2} \nabla u = \gamma^{-1/2} \sigma$, i.e., if and only if $\gamma \nabla u = \sigma$.

Let S be the set of (u, σ) characterized by

$$S = \{(u, \sigma) \mid \quad u = \phi \quad \text{on } \Gamma, \quad \nabla \cdot \sigma = 0 \quad \text{in } \Omega \quad \sigma \cdot \nu = \psi \quad \text{on } \Gamma\}.$$

Then $F = 0$ on S if and only if γ, u, and σ satisfy

$$\begin{aligned} &\nabla \cdot (\gamma \nabla u) = 0 \qquad \text{in} \quad \Omega \\ &u = \phi \quad \text{on} \quad \Gamma \\ &\gamma \frac{\partial u}{\partial \nu} = \psi \quad \text{on} \quad \Gamma \\ &\sigma = \gamma \nabla u. \end{aligned} \tag{4.2}$$

In that case, γ is a conductivity consistent with the measurements ϕ and ψ.

For $\nabla \cdot \sigma = 0$ in Ω, $u = \phi$ and $\sigma \cdot \nu = \psi$ on Γ, a simple computation gives

$$F(\gamma, u, \sigma) = \int_\Omega \gamma |\nabla u|^2 \, dx + \int_\Omega \gamma^{-1} |\sigma|^2 \, dx - 2 \int_\Gamma \phi\, \psi \, ds.$$

If more than one set of boundary measurements $\{\phi_i, \psi_i\}_{i=1}^K$ are given, then the corresponding functional would be

$$F(\gamma, \{u_i\}_{i=1}^K, \{\sigma_i\}_{i=1}^K) = \sum_{i=1}^K \int_\Omega |\gamma^{1/2} \nabla u_i - \gamma^{-1/2} \sigma_i|^2 \, dx. \tag{4.3}$$

The set S would be defined by

$$S = \{(u_i, \sigma_i)_{i=1}^K | \quad u_i = \phi_i \quad \text{on } \Gamma, \quad \nabla \cdot \sigma_i = 0 \quad \text{in } \Omega, \quad \sigma_i \cdot \nu = \psi_i \quad \text{on } \Gamma\}.$$

The reconstruction algorithm we consider seeks to minimize the functional F over S. Since

$$F(\gamma, \{u_i\}_{i=1}^K, \{\sigma_i\}_{i=1}^K) = \sum_{i=1}^K \int_\Omega \gamma |\nabla u_i|^2 \, dx + \sum_{i=1}^K \int_\Omega \gamma^{-1} |\sigma_i|^2 \, dx - 2 \sum_{i=1}^K \int_\Gamma \phi_i \, \psi_i \, ds,$$

the minimization of $F(\gamma, \{u_i\}_{i=1}^K, \{\sigma_i\}_{i=1}^K)$, for fixed γ, is equivalent to

$$\min \int_\Omega \gamma |\nabla u_i|^2 \, dx \quad \text{subject to} \quad u_i|_\Gamma = \phi_i$$

and

$$\min \int_\Omega \gamma^{-1} |\sigma_i|^2 \, dx \quad \text{subject to} \quad \nabla \cdot \sigma_i = 0, \quad \sigma_i \cdot \nu = \psi_i,$$

for all $1 \leq i \leq K$.

The above minimization is equivalent to finding the solutions of

$$\begin{aligned} &\nabla \cdot (\gamma \nabla u_i) = 0 \quad \text{in} \quad \Omega \\ &u_i = \phi_i \quad \text{on} \quad \Gamma \end{aligned} \tag{4.4}$$

and

$$\begin{aligned} &\nabla \cdot (\gamma \nabla v_i) = 0 \quad \text{in} \quad \Omega \\ &\gamma \frac{\partial v_i}{\partial \nu} = \psi_i \quad \text{on} \quad \Gamma \\ &\text{with} \quad \sigma_i = \gamma \nabla v_i, \end{aligned} \tag{4.5}$$

for all $1 \leq i \leq K$.

For fixed $\{u_i\}_{i=1}^K$ and $\{\sigma_i\}_{i=1}^K$, the minimization over $\gamma \in L^\infty(\Omega)$ can be done pointwise on the integrand

$$\sum_{i=1}^K (\gamma |\nabla u_i|^2 + \gamma^{-1} |\sigma_i|^2).$$

The result is

$$\gamma = \left(\frac{\sum_{i=1}^K |\sigma_i|^2}{\sum_{i=1}^K |\nabla u_i|^2}\right)^{1/2}, \quad \text{provided of course this is in } L^\infty(\Omega).$$

Alternating Direction Algorithm: [8], [12], [13].

1. Pick an initial guess γ.
2. For fixed γ,

   2.a Solve: $\nabla \cdot (\gamma \nabla u_i) = 0$ in Ω, $u_i = \phi_i$ on Γ, $1 \leq i \leq K$.

   2.b Solve: $\nabla \cdot (\gamma \nabla v_i) = 0$ in Ω, $\gamma \, \partial v_i / \partial \nu = \psi_i$ on Γ and set $\sigma_i = \gamma \nabla v_i$, $1 \leq i \leq K$.

3. Update γ by minimizing $F(\gamma, \{u_i\}_{i=1}^K, \{\sigma_i\}_{i=1}^K)$ for fixed $\{u_i\}_{i=1}^K$ and $\{\sigma_i\}_{i=1}^K$.
4. If the reconstruction is satisfactory, exit[1] ; else go to step 2.

This algorithm concerns scalar γ only. To build a similar algorithm to recover a matrix conductivity, the only change we have to make concerns the update of γ. We still minimize

$$F(\gamma, \{u_i\}_{i=1}^K, \{\sigma_i\}_{i=1}^K) = \sum_{i=1}^K [\int_\Omega \{(\gamma \nabla u_i)^T \nabla u_i + (\gamma - 1\sigma_i)^T \sigma_i\}\, dx - \int_\Gamma \phi_i \psi_i\, ds]$$

for fixed $\{u_i\}_{i=1}^K$ and $\{\sigma_i\}_{i=1}^K$ but the formulas are slightly more complicated:

3.a Compute $L = \sum_{i=1}^K (\nabla u_i)(\nabla u_i)^T$.
3.b Compute $M = \sum_{i=1}^K (\sigma_i)(\sigma_i)^T$.
3.c Compute eigenvalues of ML, s_1 and s_2 and corresponding eigenvectors e_1, and e_2, and set $\lambda_i = \sqrt{s_i}$, for $i = 1, 2$.
3.d Set $E = [e_1, e_2]$ and let Λ be the diagonal matrix with entries λ_1 and λ_2.
3.e Compute $X = E\Lambda E^{-1}$.
3.f Set $\gamma = XL^{-1}$

This describes the alogrithm to recover a scalar as well as a matrix conductivity.

We have tested this algorithm on several test problems and obtained somewhat promising results. In subsequent sections, we present the numerical results obtained from this algorithm.

A. Wexler et al. [12], [13] originally proposed an algorithm, which is similar to the algorithm presented here. They seek the unknown coefficient through minimization of the corresponding "residual fluxes", $\{\sigma_i - \gamma \nabla u_i\}_{i=1}^K$. They consider minimizing $\mathcal{E}$, where

$$\mathcal{E} = \int_\Omega \sum_{i=1}^K |\sigma_i - \gamma \nabla u_i|^2\, dx.$$

The idea again is that $\mathcal{E}$ is non-negative, and that if $\mathcal{E} = 0$, then the conductivity γ is consistent with the given boundary measurements.

For the numerical implementation of this algorithm we use finite element approximations to solve the boundary value problems in steps (2.a) and (2.b). We take piecewise linear test and trial functions on a uniform triangulation of the domain Ω. γ is taken to be constant on each element T_j, $j = 1, \cdots, N$. In approximating step 3 we simply minimize the functional F with fixed $\{u_i\}_{i=1}^K$ and $\sigma_i = \gamma \nabla v_i$, $1 \le i \le K$, coming from the finite

[1] We use the least squares error in our stopping criterion.

element solutions of (2.a) and (2.b). On each triangle the new value of γ (in the scalar case) is simply given by

$$\gamma_{new} = \gamma_{old} \left(\frac{\sum_{i=1}^{K} \int_{T_j} |\nabla v_i|^2 \, dx}{\sum_{i=1}^{K} \int_{T_j} |\nabla u_i|^2 \, dx} \right)^{1/2}. \tag{4.6}$$

Since u_i and v_i are piecewise linear, the integrals are not necessary and we get

$$\gamma_{new} = \gamma_{old} \left(\frac{\sum_{i=1}^{K} |\nabla v_i|^2}{\sum_{i=1}^{K} |\nabla u_i|^2} \right)^{1/2}, \quad \text{on each triangle.} \tag{4.7}$$

As a measure of how good an approximation γ_{new} is we compute the LSE(least squares error).

$$\begin{aligned} LSE &= \sum_{i=1}^{K} \Big[\int_{\Omega} \{\gamma |\nabla u_i|^2 + \gamma^{-1} |\sigma_i|^2\} \, dx - \int_{\Gamma} \phi_i \psi_i \, ds \Big] \\ &= \sum_{i=1}^{K} \Big[\int_{\Omega} \{\gamma_{new} |\nabla u_i|^2 + \gamma_{new}^{-1} |\gamma_{old} \nabla v_i|^2\} \, dx - \int_{\Gamma} \phi_i \psi_i \, ds \Big] \end{aligned} \tag{4.8}$$

(remember that $\sigma_i = \gamma_{old} \nabla v_i$).

For the anisotropic error computation, we similarly get

$$LSE = \sum_{i=1}^{K} \Big[\int_{\Omega} \{(\gamma_{new} \nabla u_i)^T \nabla u_i + (\gamma_{new}^{-1} \gamma_{old} \nabla v_i)^T (\gamma_{old} \nabla v_i)\} \, dx - \int_{\Gamma} \phi_i \psi_i \, ds \Big]. \tag{4.9}$$

5. Two–Dimensional Computation. As a test problem we consider the layered conductivity

$$\gamma(x,y) = \begin{cases} 2, & \text{if } y \geq 1/2 \\ 0.5, & \text{if } y < 1/2 \end{cases} \tag{5.1}$$

on the d· nain $\Omega = [0,1] \times [0,1]$. We seek to reconstruct this γ from three sets of boundary measurements. First we concoct three test functions $u_i, i = 1,2,3$ which satisfy

$$\nabla \cdot (\gamma \nabla u_i) = 0 \quad \text{in } \Omega$$

(across $y = 1/2$, this requires that u_i as well as its conormal derivative $\gamma \frac{\partial u_i}{\partial \nu}$ be continuous):

$$\begin{aligned} u_1(x,y) &= \begin{cases} y + 1.5, & \text{if } y \geq 1/2 \\ 4y, & \text{if } y < 1/2 \end{cases} \\ u_2(x,y) &= x \\ u_3(x,y) &= \begin{cases} xy, & \text{if } y \geq 1/2 \\ 4xy - 1.5x, & \text{if } y < 1/2. \end{cases} \end{aligned} \tag{5.2}$$

We have run the alternating direction algorithm to reconstruct the conductivity in both the isotropic and the anisotropic cases using the same three sets of boundary measurements $(u_i, \gamma \frac{\partial u_i}{\partial \nu})$.

In the actual computations to solve the boundary value problems, we use the finite element package Modulef. The regular finite element mesh is shown in figure 1. Dirichlet and Neumann boundary data are computed from the exact solutions u_i and prescribed pointwise on the boundary nodes (for Dirichlet conditions) and as an average value on the boundary edges (for Neumann conditions). The linear systems of equations are solved by Crout decomposition.

In the case of anisotropic conductors we face a problem of nonuniqueness. One way to avoid the nonuniqueness issue is to convert the matrix conductivity to an appropriate scalar. In the graphic display shown here we have simply taken $\sqrt{\det \gamma}$ as an isotropic approximation at the final stage, but we recognize that this is an ad hoc approach which is not necessarily best possible. For the graphics display, we use a grid point in each triangle, not the nodes of the original triangulation. (Figure 2 shows the grid points for the graphics.)

Figures 3 and 4 show the results of our computation. As seen both the isotropic and the anisotropic reconstructions detect some jump near the line $y = \frac{1}{2}$, though the isotropic reconstruction detects a sharper jump than the anisotropic one. Most noticably the isotropic reconstruction appears to become oscillatory after a certain number of iterations, whereas the anisotropic reconstruction displays no such oscillations and seems to improve with increasing number of iterations. This is not totally unexpected, since the reconstruction algorithm using anisotropic γ was derived from the isotropic algorithm through the elimination of highly oscillatory γ by relaxation (or G-convergence). See Kohn and Vogelius [8]. In both the isotropic and the anisotropic cases, the least squares error decreases rapidly. As seen the anisotropic reconstruction brings about smaller least squares error than the isotropic one when we compare the results at the same iterate. (See table 1.)

To examine how close the reconstruced conductivity, γ^c, is to the exact conductivity, γ^e, we have computed $\|\gamma^c - \gamma^e\|$ using both the L_1 and L_2 norms. (See figure 5 and table 2.) In this particular example, we see that the anisotropic L_1 error decreases and stays almost unchanged after about 200 iterations, while the isotropic L_1 error rapidly decreases at the very early stage of computation but starts increasing when γ becomes oscillatory (at about the 50^{th} iterate) and remains almost unchanged after about 200 iterations. The two error curves intersect at about the 120^{th} iterate, after which the isotropic L_1 error curve lies significantly above the anisotropic one. We also have computed the L_2 error and the results are qualitatively similar to those obtained using the L_1 norm, although the crossing happens at a later stage and is less dramatic.

6. One-Dimensional Computation. We now incorporate into the algorithm the fact that γ is a function of x_2 only. We take periodic boundary conditions in the x_1

direction and for simplicity we change the domain Ω to be $[0, 2\pi] \times [-1, 1]$. Assume the solution u is represented by a sine Fourier series

$$u(x_1, x_2) = \sum_{k=1}^{\infty} \alpha_k(x_2) \sin kx_1$$

(no cosine terms). To minimize $\int_\Omega \gamma |\nabla u|^2 \, dx$ is equivalent to find the solutions of

$$-(\gamma \alpha_k')' + k^2 \gamma \alpha_k = 0, \quad k = 1, 2, \cdots$$

with appropriate boundary data and to minimize $\int_\Omega \gamma^{-1} |\sigma|^2 \, dx$ subject to $\nabla \cdot \sigma = 0$ is equivalent to find the solutions of

$$-(\gamma^{-1} k^{-2} \sigma_k')' + \gamma^{-1} \sigma_k = 0, \quad k = 1, 2, \cdots$$

with appropriate boundary data. The latter follows since σ is represented as

$$\sigma(x_1, x_2) = \begin{pmatrix} \displaystyle\sum_{k=1}^{\infty} -\frac{1}{k} \sigma_k'(x_2) \cos kx_1 \\ \displaystyle\sum_{k=1}^{\infty} \sigma_k(x_2) \sin kx_1 \end{pmatrix}.$$

We seek to minimize the truncated funtional

$$(6.1) \quad F(\gamma, \{\alpha_k\}_{k=1}^K, \{\sigma_k\}_{k=1}^K) = \sum_{k=1}^{K} \int_{-1}^{1} (\gamma(k^2[\alpha_k]^2 + [\alpha_k']^2) + \gamma^{-1}(k^{-2}[\sigma_k']^2 + [\sigma_k]^2)) \, dx$$

over all α_k and σ_k with given boundary data $\alpha_k(\pm 1)$ and $\sigma_k(\pm 1)$.

The Alternating Direction Algorithm for the one–dimensional computation becomes:

1. Pick an initial guess for γ.
2. For $k = 1, \cdots, K$

   2.a Solve

   $$-(\gamma \alpha_k')' + k^2 \gamma \alpha_k = 0 \qquad \text{in } (-1, 1)$$
   $$\alpha_k(-1) \quad \text{and} \quad \alpha_k(1) \quad \text{given.}$$

   2.b Solve

   $$-(\gamma^{-1} k^{-2} \sigma_k')' + \gamma^{-1} \sigma_k = 0 \qquad \text{in } (-1, 1)$$
   $$\sigma_k(-1) \quad \text{and} \quad \sigma_k(1) \quad \text{given.}$$

3. Update γ by minimizing $F(\gamma, \{\alpha_k\}_{k=1}^K, \{\sigma_k\}_{k=1}^K)$ for fixed $\{\alpha_k\}_{k=1}^K$ and $\{\sigma_k\}_{k=1}^K$.
4. If the reconstruction is satisfactory, exit; else go to step 2.

For the numerical implementation of this one–dimensional algorithm we use piecewise linear finite elements on a uniform mesh to solve the boundary value problems (2.a) and (2.b). We implement the method as described above for two component materials. We also implement the anisotropic analogue of this algorithm based on volume fractions.

6.1 Material composed of two components. For the minimization of F we consider conductivities γ that correspond to a two component material, i.e., γ takes one of two values $\gamma^{(1)}$ or $\gamma^{(2)}$ on each element I_i, $i = 1, \cdots, N$. We seek to minimize

$$\sum_{i=1}^{N} [\gamma_i \int_{I_i} (\sum_{k=1}^{K} k^2 [\alpha_k]^2 + \sum_{k=1}^{K} [\alpha_k']^2)\, dx + \gamma_i^{-1} \int_{I_i} (\sum_{k=1}^{K} k^{-2} [\sigma_k']^2 + \sum_{k=1}^{K} [\sigma_k]^2)\, dx],$$

which amounts to minimizing

$$\gamma_i \sum_{k=1}^{K} \int_{I_i} (k^2 [\alpha_k]^2 + [\alpha_k']^2)\, dx + \gamma_i^{-1} \sum_{k=1}^{K} \int_{I_i} (k^{-2} [\sigma_k']^2 + [\sigma_k]^2)\, dx \tag{6.2}$$

on each element I_i.

We compute (6.2) with γ_i replaced by $\gamma^{(1)}$ and $\gamma^{(2)}$ respectively, compare the resulting values and select as the new conductivity the one which gives rise to the smaller energy. Step 3 may now be written:

3. For $i = 1, \cdots, N$

$$d_1 = \gamma^{(1)} \sum_{k=1}^{K} \int_{I_i} (k^2 [\alpha_k]^2 + [\alpha_k']^2)\, dx + \gamma^{(1)^{-1}} \sum_{k=1}^{K} \int_{I_i} (k^{-2} [\sigma_k']^2 + [\sigma_k]^2)\, dx$$

$$d_2 = \gamma^{(2)} \sum_{k=1}^{K} \int_{I_i} (k^2 [\alpha_k]^2 + [\alpha_k']^2)\, dx + \gamma^{(2)^{-1}} \sum_{k=1}^{K} \int_{I_i} (k^{-2} [\sigma_k']^2 + [\sigma_k]^2)\, dx \tag{6.3}$$

If $d_1 < d_2$, then $\gamma_i = \gamma^{(1)}$;
else $\gamma_i = \gamma^{(2)}$.

The least squares error is computed by summing all d_1 or d_2, whichever is smaller on each element, and finally subtracting the boundary integral.

For

$$\gamma(x) = \begin{cases} 2, & \text{for } -1 \le x \le 0 \\ 0.5, & \text{for } 0 < x \le 1, \end{cases}$$

$\alpha_k(x)$ and $\sigma_k(x)$, $1 \le k \le K$, can be computed analytically

$$\alpha_k(x) = \frac{e^{kx} + e^{-kx}}{k(e^k + e^{-k})}$$

$$\sigma_k(x) = \begin{cases} 2\, \dfrac{e^{kx} - e^{-kx}}{(e^k + e^{-k})}, & \text{for } -1 \le x \le 0 \\ 0.5\, \dfrac{e^{kx} - e^{-kx}}{(e^k + e^{-k})}, & \text{for } 0 < x \le 1. \end{cases}$$

We feed the algorithm with the exact boundary data $\alpha_k(\pm 1)$ and $\sigma_k(\pm 1)$, $1 \le k \le K$,

$$\alpha_k(-1) = \alpha_k(1) = 1/k$$
$$\sigma_k(-1) = 2\,\frac{-e^k + e^{-k}}{e^k + e^{-k}}, \quad \sigma_k(1) = 0.5\,\frac{e^k - e^{-k}}{e^k + e^{-k}}.$$

In the actual computation we take $K = 10$ and $N = 200$. We have run the alternating direction algorithm on this problem to reconstruct γ for various initial choices. In each case a new conductivity was obtained after one iteration and then it remained the same in all subsequent iterations. The least squares error changed from the first to the second iterate, since the computation of the least squares error involves γ_{old} as well as γ_{new}.

Here are some results with different initial guess.

1. Initial $\gamma = 2.0$ everywhere: the algorithm picks up a jump at $x = 0.29$ with least squares error 0.01638. Computed conductivity γ^c is: $\gamma^c = 2$ for $x < 0.29$, $\gamma^c = 0.5$ for $x > 0.29$.
2. Initial $\gamma = 0.5$ everywhere: the algorithm picks up a jump at $x = 0.29$ with least squares error 0.01638. $\gamma^c = 2$ for $x < 0.29$, $\gamma^c = 0.5$ for $x > 0.29$.
3. Initial $\gamma(x) = \begin{cases} 0.5, & \text{for } -1 \le x \le 0 \\ 2, & \text{for } 0 < x \le 1 \end{cases}$: the algorithm picks up a jump at $x = 0.58$ with least squares error 0.08429. $\gamma^c = 2$ for $x < 0.58$, $\gamma^c = 0.5$ for $x > 0.58$.
4. Initial γ = exact γ: the algorithm preserves the initial guess (jump exactly at $x = 0$) with least squares error 0.00144, the descretization error in the numerical solutions of the boundary value problems.

6.2 Volume fraction method. The method discussed in the previous section itself failed to detect the exact location of the jump discontinuity. The method would be equally unsuited to identify any oscillations in γ. We now consider a method for a two component material based on the concept of volume fractions (the anisotropic analogue of the previous method).

With a possibly highly oscillatory layered coefficient, it is well known from the theory of homogenization that the conductivity across the layers approaches the harmonic average $c = \left(\theta {\gamma^{(1)}}^{-1} + (1-\theta){\gamma^{(2)}}^{-1}\right)^{-1}$, whereas the conductivity along the layers approaches the algebraic average $m = \theta\gamma^{(1)} + (1-\theta)\gamma^{(2)}$, here θ is the so called volume fraction of material $\gamma^{(1)}$, i.e., the infinitesimal proportion of material $\gamma^{(1)}$. See Bensoussan, Lions, and Papanicolaou [2]. Clearly, $0 \le \theta(x) \le 1$ and we note that if either $\theta = 0$ or 1, then $c = m = \gamma^{(2)}$ or $\gamma^{(1)}$, respectively.

We seek to minimize the truncated functional

$$(6.4)\quad F(\theta, \{\alpha_k\}_{k=1}^K, \{\sigma_k\}_{k=1}^K) = \sum_{k=1}^{K} \int_I \left\{ c[\alpha_k']^2 + mk^2[\alpha_k]^2 + m^{-1}k^{-2}[\sigma_k']^2 + c^{-1}[\sigma_k]^2 \right\} dx.$$

We take c and m to be constant in each element I_i.

Alternating Direction Algorithm based on volume fraction θ:

1. Pick an initial guess for θ.
2. For $k = 1, \cdots, K$

   2.a Solve

$$-(c\alpha_k')' + k^2 m\alpha_k = 0 \qquad \text{in } (-1,1)$$
$$\alpha_k(-1) \quad \text{and} \quad \alpha_k(1) \quad \text{given.}$$

   2.b Solve

$$-(k^{-2}\, m^{-1}\sigma_k')' + c^{-1}\sigma_k = 0 \qquad \text{in } (-1,1)$$
$$\sigma_k(-1) \quad \text{and} \quad \sigma_k(1) \quad \text{given.}$$

3. Update θ by minimizing $F(\theta, \{\alpha_k\}_{k=1}^K, \{\sigma_k\}_{k=1}^K)$ for fixed $\{\alpha_k\}_{k=1}^K$ and $\{\sigma_k\}_{k=1}^K$.
4. If the reconstruction is satisfactory, exit; else go to step 2.

In updating θ in step (3), we minimize the nonlinear functional

$$(6.5)\quad F_i(c) = \sum_{k=1}^{K}\Big(c\int_{I_i}[\alpha_k']^2\,dx + mk^2\int_{I_i}[\alpha_k]^2\,dx + m^{-1}k^{-2}\int_{I_i}[\sigma_k']^2\,dx + c^{-1}\int_{I_i}[\sigma_k]^2\,dx\Big),$$

with respect to c on each element I_i, and we compute θ from the formula

$$\theta = (c^{-1} - {\gamma^{(2)}}^{-1})/({\gamma^{(1)}}^{-1} - {\gamma^{(2)}}^{-1}).$$

Note that F_i is a functional of c only, since m can be expressed in terms of c

$$m = \gamma^{(1)} + \gamma^{(2)} - \frac{\gamma^{(1)}\gamma^{(2)}}{c}.$$

In our computation to minimize F_i, we use Newton's method together with the Golden search rule. We take two Newton iterates. If the second iterate c_2 falls between $\gamma^{(1)}$ and $\gamma^{(2)}$, then we compare $F_i(c_2)$, $F_i(\gamma^{(1)})$, and $F_i(\gamma^{(2)})$ and choose the argument corresponding to the smallest value as the updated value for c. If the second iterate c_2 falls outside the range, then we use the Golden search algorithm (ten steps) to compute an updated value for c.

The least squares error is computed by summing the F_i's for all i and finally subtracting the boundary integral. Here we use both θ_{old} and θ_{new} in the sense that θ_{new} is used to compute F_i and θ_{old} is used to solve the boundary value problems. For our test problem we take the same exact solutions as in the previous section, i.e., $\gamma^{(1)} = 0.5$ and $\gamma^{(2)} = 2$, and in terms of volume fraction

$$\theta(x) = \begin{cases} 0, & \text{for } -1 \le x \le 0 \\ 1, & \text{for } 0 < x \le 1. \end{cases}$$

We have run the algorithm on this problem to reconstruct θ (again with $K = 10$, $N = 200$ and exact boundary data) with various choices of initial guess; the results however are almost independent of initial guess. This method reconstructs θ fairly well succeeding to detect the jump discontinuity. Figure 6 shows the results obtained from this method with initial guess $\theta = 0.5$. The least squares error decreases very rapidly at the very early stages of the computation. We have also computed $\|\theta^c - \theta^e\|_{L^1}$, where θ^c is the reconstructed volume fraction and θ^e is the exact volume fraction. (See table 3.) As seen the L^1 error decreases as the number of iterations increases.

We have tested the same problem on meshes of various dimensions. Figure 7 shows the reconstruction results when $N = 25$. We see that the least squares error is much smaller when N is larger. For example, the least squares error when $N = 25$ is 0.07249 at the 50^{th} iterate while it is 0.00122 when $N = 200$ at the same iterate. Surprisingly enough, the L_1 error is smaller when N is smaller. For example, the L_1 error when $N = 25$ is 0.05641 at the 50^{th} iterate while it is 0.0.08921 when $N = 200$ at the same iterate. This is a phenomenon which we have come across in several of the computations – basically it asserts that there is nothing to be gained (occasionally something to be lost) by using a too fine mesh to identify a simple discontinuous coefficient. See figure 8 and table 3 for the comparison of the least aquares errors and the L_1 errors.

6.3 Perturbed data. Let us consider a problem to reconstruct θ, slightly perturbed from the one in the previous section, i.e., a problem which corresponds to the exact θ

$$\theta(x) = \begin{cases} -\frac{1}{2}x - \frac{1}{4}, & \text{for } -1 \le x \le -0.5 \\ 0, & \text{for } -0.5 < x \le 0 \\ 1, & \text{for } 0 < x \le 0.5 \\ -\frac{1}{2}x + \frac{5}{4}, & \text{for } 0.5 < x \le 1. \end{cases}$$

We do not compute the boundary data analytically for this problem. Instead we set $\alpha_k(\pm 1) = 1/k$ for $k = 1, \cdots, K$ and solve the boundary value problems

$$\begin{aligned} -(c\alpha_k')' + mk^2\alpha_k &= 0 \qquad \text{in } (-1,1) \\ \alpha_k(-1) = \alpha_k(1) &= 1/k \end{aligned} \tag{6.6}$$

numerically, using piecewise linear finite elements on a mesh with $N = 800$. As data for σ_k, we use

$$\begin{aligned} \sigma_k(-1) &= c(-1)\,\alpha_{k,h}'(-1) \\ \sigma_k(1) &= c(1)\,\alpha_{k,h}'(1), \end{aligned}$$

where $\alpha_{k,h}'(x)$ is the finite element approximation of $\alpha_k'(x)$.

We have run the Alternating Direction Algorithm based on volume fractions on this problem. The reconstruction results are shown in figure 9 and table 4 with initial guess

$\theta = 0.5$. Almost the same conclusions can be drawn from this computation as in the case of the previous problem except that the L^1 error is larger for smaller N in this case.

Here are some observations:

1. The algorithm reconstructs θ fairly well with reasonably small least squares error.
2. The results are almost independent of initial guess for θ.
3. The least squares error decreases rapidly as N gets larger when compared at the same iterate.
4. The L_1 error in the computed volume fraction decreases as the number of iterations increases.

For comparison, we tried the algorithm in section 6.1 on this problem to see whether it would detect any oscillations. It picked up a single jump after one iteration and the solution remained the same in all subsequent iterations. The location of the computed jump depends on the initial choice of γ, however the method failed to pick up any oscillations. The location of jump is slightly different from the one in section 6.1 with the same initial guess; the least squares error is naturally much bigger. For example, with the initial guess $\gamma = 0.5$ everywhere, the algorithm picked up a jump at $x = 0.25$, i.e., $\gamma^c = 2$ for $x < 0.25$, $\gamma^c = 0.5$ for $x > 0.25$ with least squares error 0.43973.

6.4 Piecewise quadratic finite elements. As seen we have obtained quite satisfactory reconstructions of θ in the previous two sections. To analyze the effect of higher accuracy we also tried to use piecewise quadratic finite elements in solving the boundary value problems (2.a) and (2.b). The coefficients c and m are treated as piecewise linear (not necessarily continuous). In the step to update θ it might seem natural to minimize over all piecewise linear θ. This however produces a very complicated updating step. Instead we have decided to use one of the following two options : (1) keep θ piecewise constant as before, or (2) minimize the functional with respect to θ pointwise at the nodes of each element and let θ elementwise be the linear interpolation (not necessarily continuous).

We have run the Alternating Direction Algorithm based on the volume fractions on the problems of section 6.2. Figure 10 and table 5 show the results of this computation. In our first computations we reconstructed the volume fractions using option (1). The results are almost the same as with piecewise linear elements in the sense of L_1 error, of course the least squares error is significantly reduced. In the actual computation of the problem, we got a negative least squares error in the computation with $N = 200$; this is due to round–off error. We computed the same problem in double precision, which brought about a very small, but positive least squares error.

We have also used option (2) on the same problem. The results look reasonable except near the jump discontinuity. This is not unexpected since the minimization of the functional requires pointwise approximations to the derivatives of the solutions to the boundary value problems. These approximations are clearly not very good near the jump discontinuity.

Finally we computed with the perturbed data from section 6.3. We used option (1) – the results are shown in figure 10 and table 6.

In summary it seems that the increased accuracy in the finite element solutions has very little effect on the L_1 error of the computed solutions. Based on this observation and considerations regarding simplicity, it seems entirely reasonable to solve the finite element problems using only piecewise linears. We do not know whether this conclusion is also valid for more smoothly varying θ. In that case one might suspect that higher accuracy could improve the L_1 error.

REFERENCES

[1] G. ALESSANDRINI, *Stable determination of conductivity by boundary measurements*, IMA Tech. Report 1987.

[2] A. BE[illegible]USSAN, J. L. LIONS AND G. PAPANICOLAOU, *Aymptotic Analysis for Periodic Structures*, North Holland Pub. Co., Amsterdam · New York · Oxford, 1978.

[3] A. P. CALDÉRON, *On an inverse boundary value problem, Seminar on Numerical Analysis and its application to Continuum Physics*, Soc. Brasileira de Matemática, Rio de Janeiro, 1980.

[4] A. FRIEDMAN AND M. VOGELIUS, *Identification of small inhomogeneities of extreme conductivity by boundary measurements: a continuous dependence result*, Arch. Rat. Mech. Anal. (to appear).

[5] R. KOHN AND M. VOGELIUS, *Identification of an unknown conductivity by means of measurements at the boundary*, SIAM-AMS Proceedings, 14 (1984), pp. 113–123.

[6] R. KOHN AND M. VOGELIUS, *Determining conductivity by boundary measurements*, Comm. Pure Appl. Math, 37 (1984), pp. 289–298.

[7] R. KOHN AND M. VOGELIUS, *Determining conductivity by boundary measurements II. Interior results*, Comm. Pure Appl. Math, 38 (1985), pp. 643–667.

[8] R. KOHN AND M. VOGELIUS, *Relaxation of variational method for Impedance Computed Tomography*, Comm. Pure Appl. Math, 40 (1987), pp. 745–777.

[9] J. SYLVESTER AND G. UHLMANN, *A uniqueness theorem for an inverse boundary value problem in electrical prosepection*, Comm. Pure Appl. Math, 39 (1986), pp. 91–112.

[10] J. SYLVESTER AND G. UHLMANN, *A global uniqueness theorem for an inverse boundary value problem*, Annals of Math., 125 (1987), pp. 153–169.

[11] J. SYLVESTER AND G. UHLMANN, *Inverse boundary value problems at the boundary - continuous dependence*, Comm. Pure Appl. Math (to appear).

[12] A. WEXLER, B. FRY AND M. R. NEUMANN, *Impedance computed tomography algorithm and system*, Appl. Optics, 24 (1985), pp. 3985–3992.

[13] A. WEXLER AND C. J. MANDEL, *An impedance computed tomography algorithm and system for ground water and hazardous waste imaging*, presented to the 2^{nd} Annual Canadian/American Conf. on Hydrogeology, Banff, June, 1985.

Figures and Tables

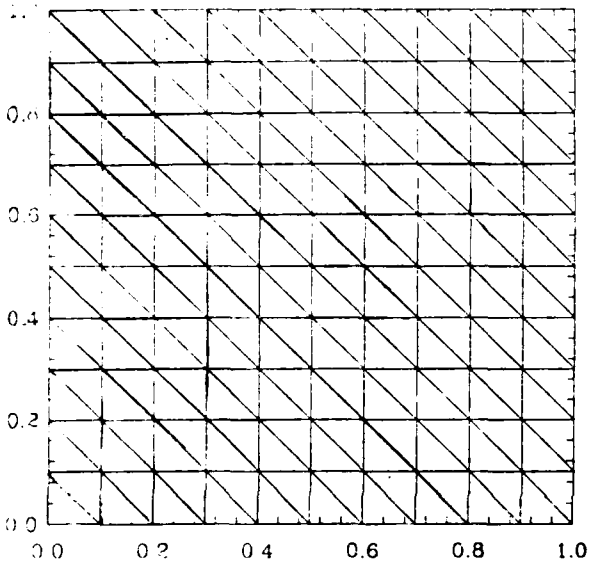

Figure 1

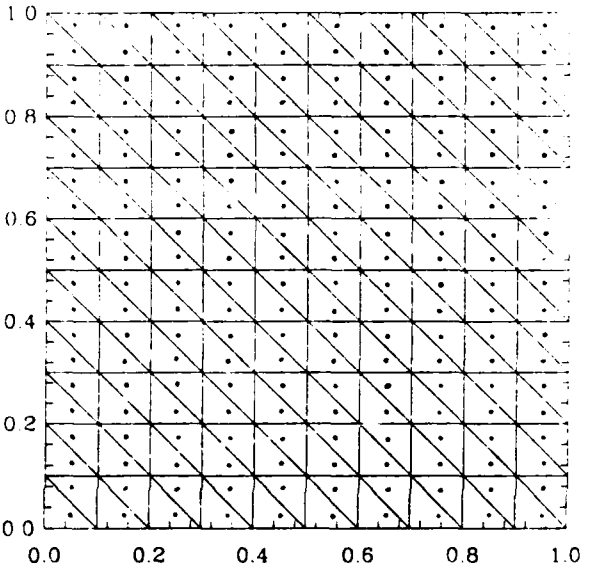

Figure 2

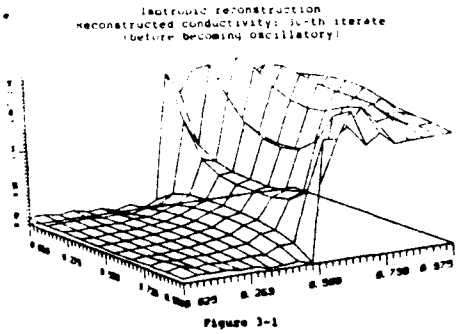

Figure 3-1

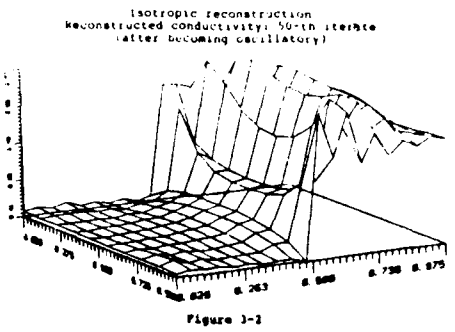

Figure 3-2

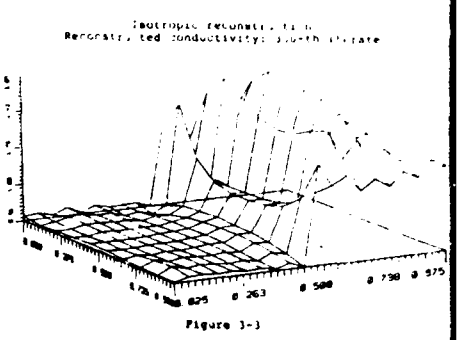

Figure 3-3

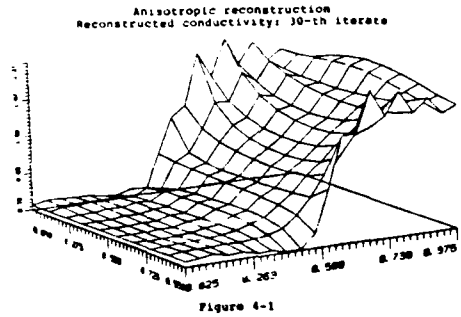

Figure 4-1

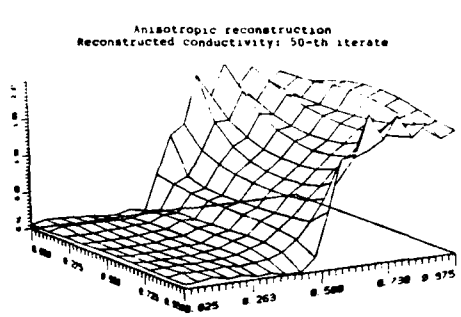

Figure 4-2

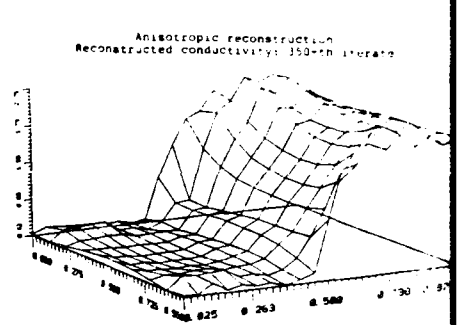

Figure 4-3

Table 1

number of iterations	least squares error (isotropic)	least squares error (anisotropic)
1	0.43236	0.26953
5	0.00781	0.00181
10	0.00496	0.00081
20	0.00274	0.00056
30	0.00161	0.00044
40	0.00109	0.00037
50	0.00081	0.00033
100	0.00033	0.00024
150	0.00023	0.00019
200	0.00022	0.00015
250	0.00019	0.00011
300	0.00019	0.00010
350	0.00019	0.00010

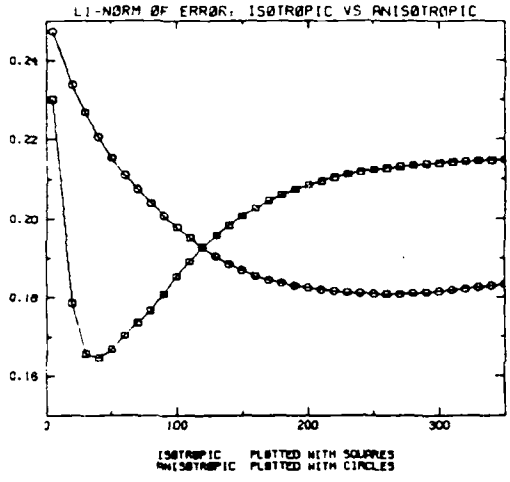

Figure 5-1

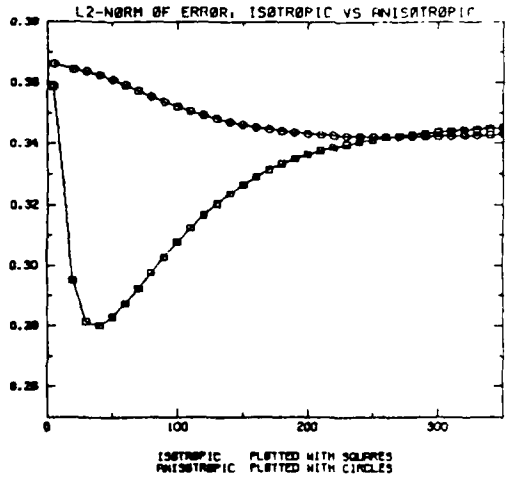

Figure 5-2

Table 2

number of iterations	L1 error (isotropic)	L1 error (anisotropic)	L2 error (isotropic)	L2 error (anisotropic)
5	0.230062	0.247373	0.3588591	0.366115
20	0.178497	0.233846	0.295077	0.364288
50	0.166697	0.215210	0.283006	0.360893
100	0.185301	0.197864	0.307787	0.352130
150	0.200615	0.186805	0.326579	0.346145
200	0.208475	0.182351	0.336369	0.343204
250	0.212179	0.180737	0.341201	0.342213
300	0.213886	0.181449	0.343713	0.342388
350	0.214690	0.183172	0.345156	0.34012

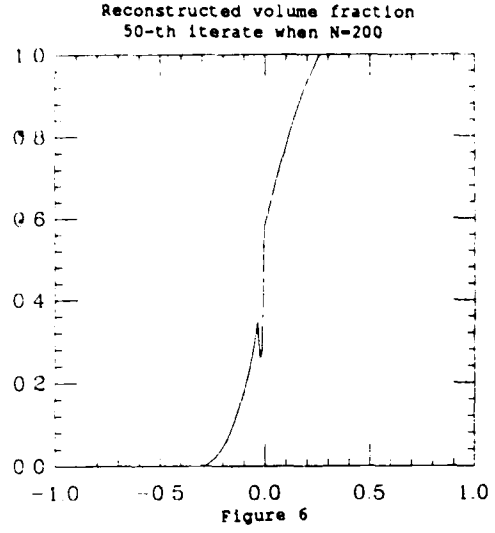

Figure 6

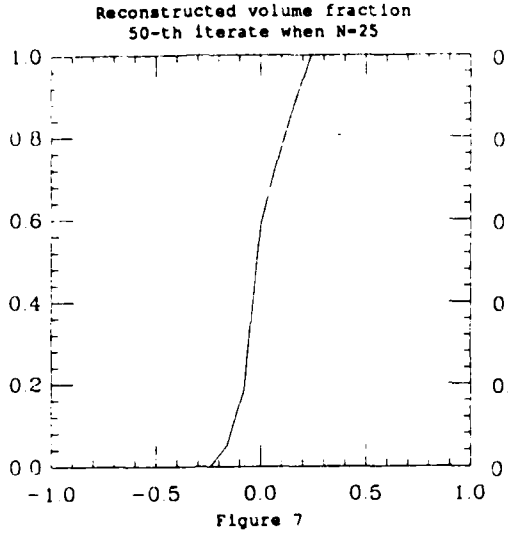

Figure 7

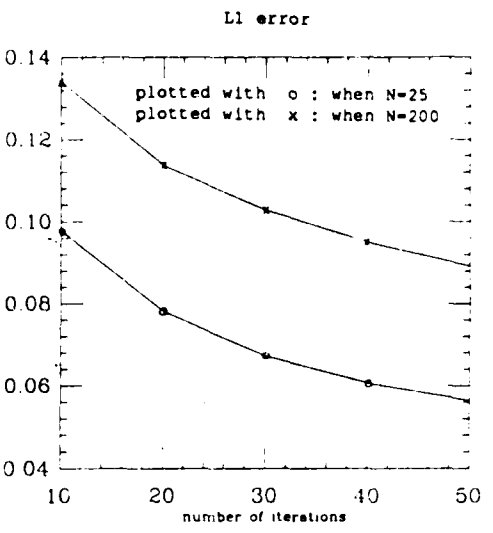

Figure 8

Table 3

number of iterations	least squares error (N=25)	least squares error (N=200)	L_1error (N=25)	L_1error (N=200)
10	0.07325	0.00199	0.09785	0.13418
20	0.07271	0.00144	0.07809	0.11360
30	0.07257	0.00131	0.06726	0.10274
40	0.07252	0.00125	0.06066	0.09508
50	0.07249	0.00122	0.05641	0.08921

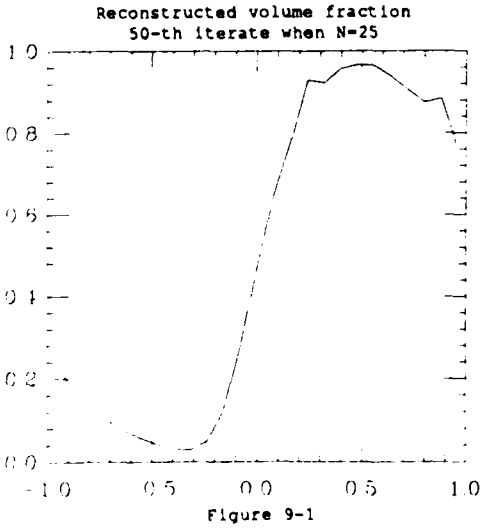

Figure 9-1

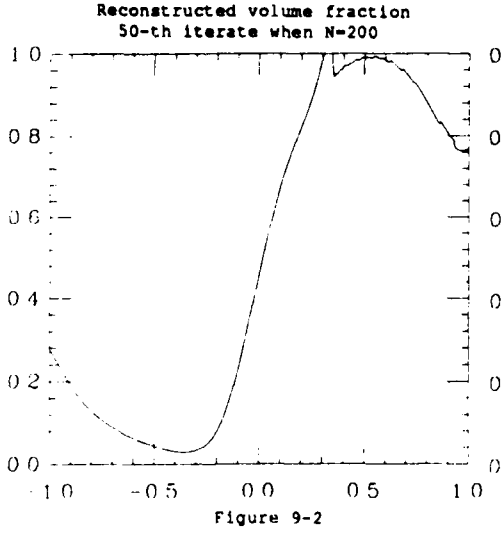

Figure 9-2

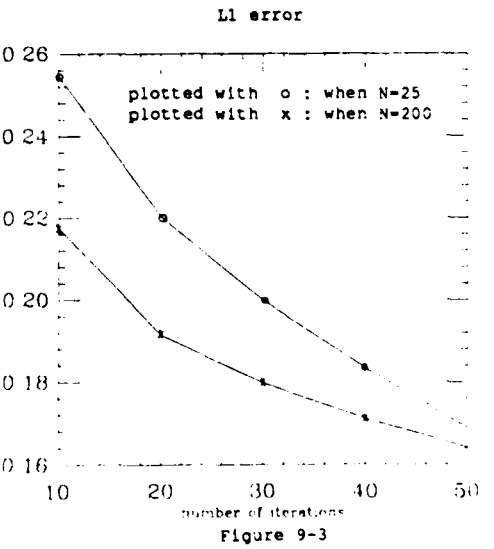

Figure 9-3

Table 4

number of iterations	least squares error (N=25)	least squares error (N=200)	L_1error (N=25)	L_1error (N=200)
10	0.08502	0.00246	0.25482	0.21760
20	0.08439	0.00169	0.22025	0.19148
30	0.08417	0.00156	0.19988	0.17979
40	0.08403	0.00148	0.18331	0.17110
50	0.08392	0.00144	0.16895	0.16420

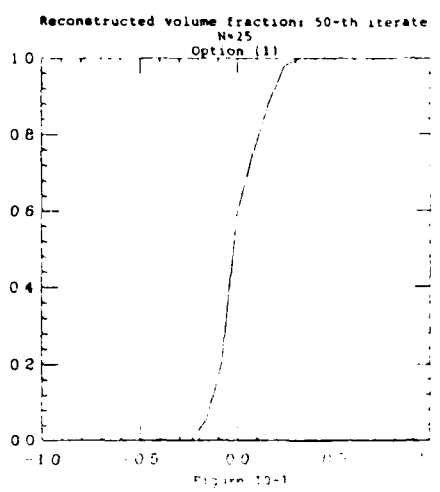

Figure 10-1

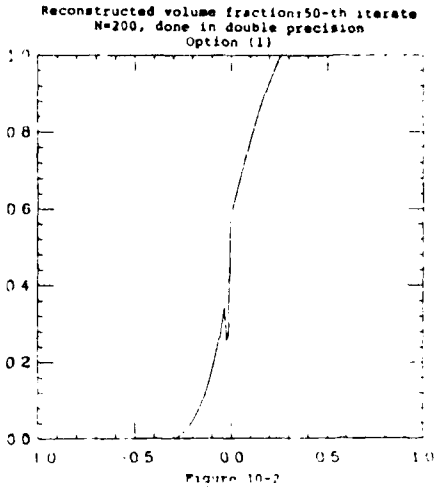

Figure 10-2

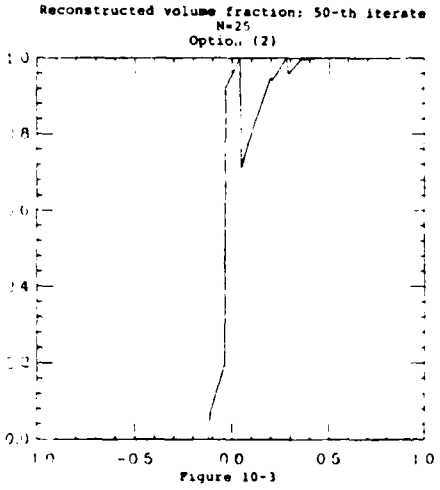

Figure 10-3

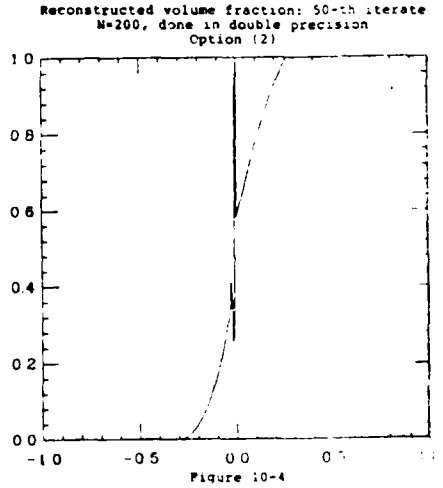

Figure 10-4

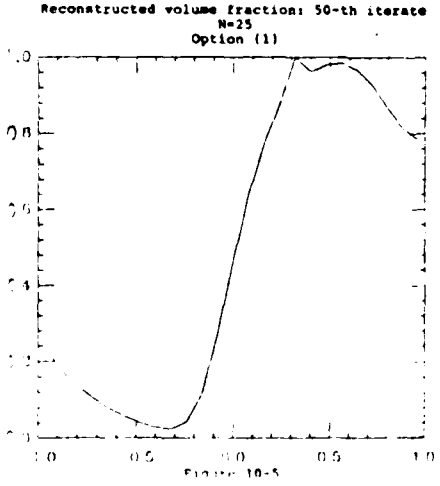

Figure 10-5

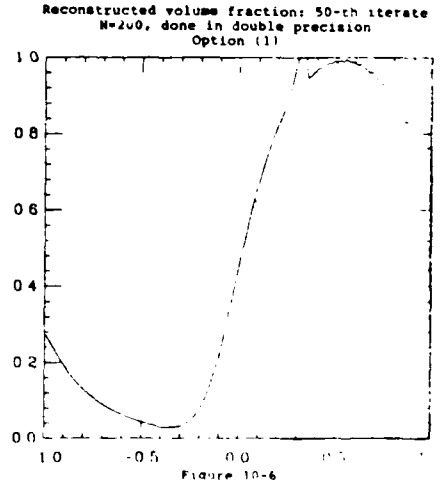

Figure 10-6

Table 5: Piecewise quadratic finite element results on problem in section 6.2

When option (1) is used:

number of iterations	least squares error (N=25) (single precision)	least squares error (N=200) (double precision)	L_1error (N=25) (single precision)	L_1error (N=200) (double precision)
10	0.00116	0.00091	0.11987	0.13418
20	0.00067	0.00031	0.10005	0.11362
30	0.00055	0.00017	0.08851	0.10275
40	0.00050	0.00011	0.07993	0.09509
50	0.00047	0.00008	0.07331	0.08921

When option (2) is used

number of iterations	least squares error (N=25) (single precision)	least squares error (N=200) (double precision)	L_1error (N=25) (single precision)	L_1error (N=200) (double precision)
10	0.00344	0.00105	0.11689	0.13454
20	0.00276	0.00043	0.09963	0.11525
30	0.00213	0.00027	0.09254	0.10544
40	0.00167	0.00020	0.08457	0.09858
50	0.00155	0.00015	0.07799	0.09327

Table 6: Piecewise quadratic finite element results on problem in section 6.3

number of iterations	least squares error (N=25) (single precision)	least squares error (N=200) (double precision)	L_1error (N=25) (single precision)	L_1error (N=200) (double precision)
10	0.00326	0.00129	0.20264	0.21753
20	0.00174	0.00039	0.17177	0.19132
30	0.00162	0.00025	0.15869	0.17944
40	0.00144	0.00019	0.14894	0.17061
50	0.00140	0.00012	0.14094	0.16356